



# The peak shape model for magnetic sector and time-of-flight mass spectrometers

Oleg N. Peregodov\*, Oleksandr M. Buhay

*Institute of Applied Physics, National Academy of Sciences of Ukraine, 58 Petropavlivska Str., 40000 Sumy, Ukraine*

## ARTICLE INFO

### Article history:

Received 8 April 2010

Received in revised form 3 June 2010

Accepted 9 June 2010

Available online 29 June 2010

### Keywords:

Peak shape model

Peak fitting

Quantitative analysis

Mass spectrometry

## ABSTRACT

A general approach to model peak shapes of magnetic sector and time-of-flight (TOF) mass spectrometers is described. The peak shape model is based on the physical principles of the signal formation in the detector and contains five parameters: the peak area, the peak position on the mass scale, the estimate of peak width and the degree of asymmetry of the peak. The last parameter characterizes the relative increment of the ion bending radius (magnetic sector instrument) or the relative time channel width of the detector (TOF mass spectrometer). The model can be used for computer processing of mass spectra, e.g., for the separation of partially overlapped peaks, for comparison of the peaks recorded under different conditions of ionization, estimation of peak areas, etc.

© 2010 Elsevier B.V. All rights reserved.

## 1. Introduction

In mass spectrometry, as in many other analytical techniques, the information concerning a physical or chemical quantity has to be extracted from a peak-shaped signal superimposed on a background contaminated with noise [1]. The problems involved in extracting the information reliably depend on the complexity of the signal, on the prior knowledge about the system, and, of course, on the information required.

It is known that the mass spectrometer can measure only two values: the mass-to-charge ratio and the abundance ratio of the ions. These two basic values are the initial data in problems of identification of the unknown substances [2,3], determination of their elemental composition (chemical formula) [4–7], creation and effective use of the unified databases of the organic compounds [8–10], and in other applications. Additional parameters (peak width, peak area, etc.) could be necessary for specific tasks [11,12].

Modern mass-spectrometric systems can perform tens and hundreds of analysis in the automatic mode. Handling a large volume of the obtained experimental data requires significant computational resources. This stimulates many authors to develop and improve methods, algorithms and software for mass spectra processing [5,8,12–18].

To date, there is a choice between the commercial software packages supplied by the developers of the mass spectrometer systems and free academic projects based on the open source con-

cepts [12,16,19]. The algorithms used in the commercial software are often not known to the public and the parameters that govern their behavior are rarely accessible. On the other hand, open source projects are described in details.

Typical mass spectra processing algorithm consist of several successive stages: selection and compensation of baseline, filtering the noise, detection of the peaks and their fitting with sufficient models and approximations in order to obtain the required information.

From the works [18–21] it could be concluded that there is a need in developing general mathematical models for the description of baseline and noise which are always present in mass spectra. For example, some variants of the baseline distortion were analyzed in protein mass spectra [15,22]. The authors presented the model of the baseline as a superposition of constant value and exponential series decreased with time. Such a model reasonable describes distortion of the baseline caused by the charge accumulation effects and the detector saturation. The model is applicable for TOF mass spectrometers with the analog detector.

In case of counting detector (e.g., time-to-digital converter or ion counter), statistical properties of the noise is described by the Poisson distribution. This information can be used in mass spectra processing [13,14]. Such a model was used in the investigation of the noise influence on the deisotoping of proteins and peptides [21]. The model has been tested using the data of electro-spray quadrupole time-of-flight (Q-TOF) and ion trap instruments. The authors note, that their model explains most of the observed noise, although a fraction of noise of the unknown source is always present in mass spectra, and hence noise model requires future refinement. Moreover, this model cannot be used for analog detectors [18].

\* Corresponding author. Tel.: +380 686516499; fax: +380 542223760.  
E-mail address: [o.peregodov@gmail.com](mailto:o.peregodov@gmail.com) (O.N. Peregodov).

According to Ref. [20], there is no generally accepted peak shape model of the separate mass-spectrometric peaks. From the experimental results we can state that in general case for magnetic sector and TOF mass spectrometers the shape of the peak can be represented by an asymmetric function with one maximum. In case of magnetic sector instruments the peak shape with a flat top is frequently observed.

Knowledge of the peak shape is necessary for building of the matching filters [14,15,23], selecting adequate wavelet transform [18,20,24], and fitting of the experimental data by the least-squares for obtaining quantitative values (peak position on the mass scale, intensity, etc.) [25,26].

There are several mathematical models for separate mass spectral peaks approximation [20,23,25–28]. The choice of a particular model usually done to cheapness of computation efforts, and not always the parameters of the model have physical meaning.

For example, Zubarev et al. [27] proposed the peak shape model for TOF particle desorption mass spectrometry in the form of convolution of the Gaussian with the exponent:

$$F(z) = \int_0^{\infty} e^{-(t/\alpha)} e^{-((t-z)^2/2\sigma^2)} dt,$$

where  $F(z)$  is the observed peak shape,  $\alpha$  is the parameter which characterizes both the time of ion formation and average energy deficit and  $\sigma$  is the dispersion of the Gaussian curve in the absence of the energy deficit (instrumental response). The authors suggest that the ideal peak has the shape of the Gaussian distribution. The model accounts for effect of the later ions formation in the gas phase and hence, correction of a peak position on the mass scale could be done. However, the procedure for determining the parameters of the model suitable for practical use is not described.

The peak shape model for magnetic sector mass spectrometer in the form of convolution used in [28]:

$$I(t) = \int_{-\infty}^{\infty} \phi(t - \tau) i(\tau) d\tau,$$

where  $I(t)$  is the recorded signal of the mass spectrometer,  $\phi(t)$  is the impulse response function, which describes the dynamic processes in data acquisition channel of the mass spectrometer and  $i(t)$  is the true peak shape. Two types of impulse response functions are considered and both of them lead to solutions with oscillations on the peak tails. This fact makes further signal processing and analysis more complex. The disadvantages of this work are the lack of clear criteria for the selection of impulse response functions.

In works [25,26] the peak shape model is presented as a sum of two Gaussian functions which are shifted relative to each other on the mass scale by a small value. The model has been used for TOF mass spectra processing and the accuracy of determination the peak position on the mass scale claimed to be improved. The shift value is determined empirically, and the physical meaning of the model parameters has not been explained.

Another approach is to describe the separate peaks by Gaussian and Lorentz (Cauchy) functions and their linear combinations [20,29,30].

It is worth to mention the quasi-spline approximation method [31,32] for fitting of the peak shape with piecewise continuous polynomials. This approach is applicable for mass spectra processing of magnetic sector and TOF mass spectrometers equipped with counting detectors. The necessity of mass spectra pre-smoothing and manual selection of the approximation parameters are the main disadvantages of the quasi-spline approximation method.

In present study we extended the previously proposed peak shape model of the magnetic sector mass spectrometers [33,34] to the TOF instruments and developed a general peak shape model for these types of mass spectrometers. The main requirements for pro-

posed model were account for the basic physical principles of the signal formation on the mass spectrometer detector and adequate description of the experimental signal (in terms of minimum sum of squared residuals). Also an attempt was made to show experimentally the relation of the model parameters with the physical processes affecting the ion formation in the ion source of the TOF mass spectrometer.

## 2. Experiment

To test the developed model the experiments were performed on the MALDI-TOF mass spectrometer Autoflex II (Bruker Daltonics, Germany) equipped with a nitrogen laser ( $\lambda = 337$  nm) with FlexControl 2.2 software (Bruker Daltonics, Germany).

Cesium iodide (CsI) obtained from Sigma–Aldrich was selected as a sample due to the fact that it gives a simple mass spectrum which contains the only peak corresponding to the  $\text{Cs}^+$  ions. This makes possible directly to observe dependence of the peak shape on the ion source parameters, which was the main aim of the experiments.

Aqueous solution of CsI in volume  $1 \mu\text{l}$  was deposited on the standard substrate made of stainless steel. The sample was placed into the ion source of the mass spectrometer after complete drying. Intensity of the laser was set to 50%, sample rate – 2 GS/s, pulsed ion extraction delay – 10 ns, Uis1 – 20 kV, Uis2 – 18.75 kV, lens – 7.40 kV. Linear mode of mass separation for positive ions was used. Spectra were summed for 10 different points of 10 laser shots in each point.

To demonstrate the efficiency of the presented model in separation of partially overlapped peaks we use mass spectrum of fullerenes  $\text{C}_{60}$  (Merck).  $1 \mu\text{l}$  of a saturated solution of fullerenes in toluene ( $\text{C}_6\text{H}_5\text{CH}_3$ ) was deposited on a standard substrate. The sample was placed into the ion source of the mass spectrometer after complete drying of the solvent. The positive ions spectra were recorded in linear mode of mass separation with the time of delayed extraction of 100 ns.

## 3. Computational theory and methods

### 3.1. The peak shape model for magnetic sector mass spectrometer

Integral peak recorded by the detector of the mass spectrometer in general case can be represented as a convolution

$$I(\tilde{m}) = \int_0^{\infty} K(\tilde{m} - x) f(x) dx, \quad (1)$$

where  $I(\tilde{m})$  is the recorded signal of the mass spectrometer,  $\tilde{m} = m/z$  is the mass-to-charge ratio of ions,  $f(x)$  is the function of the density distribution of ions in the beam cross section and  $K(x)$  is the impulse response function of the detector slit.

As the impulse response function of the detector slit one can use the rectangular function given, for example, by the product of two Heaviside step functions:

$$K(x) = H(x - \mu + s) H(-x + \mu + s), \quad (2)$$

where  $H(x)$  is the Heaviside step function,  $\mu$  is the coordinate of the center of the detector slit and  $s$  is the half-width of the detector slit.

Substituting (2) in (1) and taking into account the definition of the step function we obtain:

$$I(\tilde{m}) = \int_{\tilde{m}-s}^{\tilde{m}+s} f(\tau - \mu) d\tau. \quad (3)$$

Thus, integral peak recorded by the mass spectrometer is the result of integrating the source peak, which is a function of the

density distribution of ions in the beam cross section within the detector slit [33].

The solution of Eq. (1), i.e. reconstruction of function of the density distribution  $f(x)$  from the registered signal of mass spectrometer  $I(\tilde{m})$ , belongs to a class of inverse ill-posed in the sense of Hadamard problems [35,36]. The problem becomes ill-posed due to the fact that the left side of equation (1) is always recorded with an error  $\nu(\tilde{m})$ . The presence of this error as well as relative errors in the kernel  $K(x)$  and errors of the solution methods can lead to larger errors so that the numerical solution (e.g., obtained by a quadrature method) will not have anything to do with the exact one. The instability also arises in the solution of Eq. (1) obtained by the method of eigenfunctions, the projection methods and the Fourier transform method [36].

Known so far stable methods for solving Eq. (1) are based on additional *a priori* information [35–37], namely: statistical properties of the measurement error  $\nu(\tilde{m})$  and additional information about the solution  $K(x)$ .

Based on the introduction of this work, we can conclude that in general formulation the statistical characteristics of noise are not known. As for the function of the density distribution, then based on experimental data and results of computer simulation of ion sources and mass analyzers [38–41] we can conclude that in general case this is an asymmetric unimodal distribution. In our previous works [33,34], we used the Gaussian modified according to Fraser and Suzuki [42] as the distribution function:

$$f_{FS}(\tilde{m}) = \frac{1}{\sqrt{2\pi}\sigma} \exp\left(-\frac{\ln^2(1+k(\tilde{m}/\sqrt{2}\sigma))}{k^2}\right), \quad (4)$$

where  $\sigma$  is the parameter characterizing the width of the peak and  $k$  is the dimensionless parameter, characterizing the peak asymmetry degree.

Using (4) we can write the peak shape model of the separate peak of magnetic sector mass spectrometer:

$$I(\tilde{m}) = \frac{A}{\sqrt{2\pi}\sigma} \int_{\tilde{m}-s}^{\tilde{m}+s} \exp\left(-\frac{\ln^2(1+k((\tau-\mu)/\sqrt{2}\sigma))}{k^2}\right) d\tau, \quad (5)$$

where  $A$  is the peak area.

Adequacy of the model (5) and physical meaning of the parameters  $A$ ,  $s$  and  $\sigma$  for magnetic sector mass spectrometers have been confirmed experimentally [33].

Developing model (5) we assumed [33] that the width of the collector slit in  $m/z$  units is a constant value ( $s = \text{const}$ ). This is quite a good approximation, but, in real experiments, the value of the collector slit width in  $m/z$  units is not constant and depends on the current mass. This fact must be considered for more precise description of partially overlapped signals. It was shown [34], that half-width of the collector slit, expressed in  $m/z$  units, can be determined from the geometry of the mass analyzer. Taking into account a variable width of the collector slit we can rewrite the peak shape model for magnetic sector mass spectrometers as:

$$I(\tilde{m}) = \frac{A}{\sqrt{2\pi}\sigma} \exp(k^2/4) \times \int_{\tilde{m}(1-\rho^2-2\rho)}^{\tilde{m}(1+\rho^2+2\rho)} \exp\left(-\frac{\ln^2(1+k((\tau-\mu)/\sqrt{2}\sigma))}{k^2}\right) d\tau, \quad (6)$$

where  $\rho$  is the dimensionless parameter, which characterizes the relative increment of the ion bending radius that match half-width of the collector slit expressed in  $m/z$  units. For magnetic sector mass spectrometer, in contrast to the parameter  $s$ , the value  $\rho$  is constant for a given mass spectrum, which confirmed experimentally [34].

The initial value of the parameter  $\rho$  in the approximation of the experimental signals by model (6) can be determined by the formula:

$$\rho = \sqrt{1 + \frac{s}{\tilde{m}}} - 1. \quad (7)$$

### 3.2. The peak shape model for TOF mass spectrometer

In TOF mass spectrometer flight time of ions is calculated as [43]:

$$t = \frac{L_{\text{eff}}}{\sqrt{2eU_{\text{acc}}}} \sqrt{\tilde{m}} = a\sqrt{\tilde{m}}, \quad (8)$$

where  $e$  is the charge of an electron,  $L_{\text{eff}}$  is the effective length of the TOF analyzer and  $U_{\text{acc}}$  is the full accelerating voltage in the TOF. The effective length of the TOF analyzer takes into account the longer residence time in the electrostatic mirror and accelerating column. Typically, the flight time of the ion is recorded on the leading edge of the pulse in the detector. The value  $a$  is a constant for a given mass spectrum.

Each TOF acceleration pulse results in a spectrum of arrival times, and these individual spectra are summed in memory over the course of the acquisition period, forming a mass spectrum which is a histogram of the events from several pulses. If we consider each individual bin of the histogram as an analog of the collector slit of the magnetic sector mass spectrometer then all the arguments concerning the principles of the signal formation in the magnetic instrument would be applicable for TOF mass spectrometers. The only difference will be the choice of integration limits in Eq. (3), which in the case of TOF mass spectrometer can be written as:

$$I(\tilde{m}) = \int_{\tilde{m}}^{\tilde{m}+s} f(\tau - \mu) d\tau. \quad (9)$$

In contrast to the magnetic sector mass spectrometer, where the half-width of the collector slit  $s$  in general case is unknown, in the TOF instrument parameter  $s$  can be expressed by the time channel width of the detector  $\Delta t$ :

$$\Delta t = a(\sqrt{\tilde{m}+s} - \sqrt{\tilde{m}}), \quad (10)$$

where  $s$  is the time channel width of the detector expressed in  $m/z$  units. Usually, the value  $a$  is a constant during the mass spectrum recording.

By analogy with the magnetic mass spectrometer, let us define the value of the relative time channel width of the detector for the TOF instrument using (10) and (7):

$$\rho = \frac{\Delta t}{a\sqrt{\tilde{m}}}. \quad (11)$$

In this expression the coefficient  $\Delta t/a$  can be determined, for example, from the recorded mass spectrum using Levenberg–Marquardt method and Eq. (10). The value of  $\rho$  will be used for the direct calculation of the upper limit of integration in the peak shape model of the TOF mass spectrometer:

$$I(\tilde{m}) = \frac{A}{\sqrt{2\pi}\sigma} \exp(k^2/4) \times \int_{\tilde{m}}^{\tilde{m}(1+\rho^2+2\rho)} \exp\left(-\frac{\ln^2(1+k((\tau-\mu)/\sqrt{2}\sigma))}{k^2}\right) d\tau. \quad (12)$$

From Eq. (11) one can see that the parameter  $\rho$  is not constant for TOF mass spectrometers (in contrast to magnetic sector devices) and decreases in proportion to  $1/\sqrt{\tilde{m}}$ . On the other hand the time

channel width of the detector expressed in  $m/z$  units increases in proportion to  $\sqrt{\tilde{m}}$ :

$$s(\tilde{m}) = \tilde{m} (\rho^2 + 2\rho) = \frac{\Delta t}{a} \left( \frac{\Delta t}{a} + 2\sqrt{\tilde{m}} \right). \quad (13)$$

The model (6) and (12) fully satisfy the condition of normalization of the integrand area, i.e.

$$\frac{1}{\sqrt{2\pi}\sigma} \int_{-\infty}^{\infty} \exp\left(-\frac{\ln^2\left(1+k\left(\frac{\tau-\mu}{\sqrt{2}\sigma}\right)\right)}{k^2}\right) d\tau = 1. \quad (14)$$

As was shown [13], if condition (14) holds, then the area  $A$  will be an efficient estimate of the peak intensity. We confirm this fact experimentally by measuring isotopic ratios of krypton [34].

Proposed model can be used for the separation of partially overlapped peaks. In this case the model (12) can be represented as:

$$I(\tilde{m}) = \int_{\tilde{m}}^{\tilde{m}(1+\rho^2+2\rho)} \sum_{i=1}^{N_p} \frac{A_i}{\sqrt{2\pi}\sigma_i \exp(k_i^2/4)} \times \exp\left(-\frac{\ln^2\left(1+k_i\left(\frac{\tau-\mu_i}{\sqrt{2}\sigma_i}\right)\right)}{k_i^2}\right) d\tau. \quad (15)$$

where  $N_p$  is supposed number of peaks in the multiplet.

While the numerical calculation of definite integrals in the model (6) or (12) an overflow may occur in cases when the intensities in the mass spectrum exceed a few tens of units by the absolute value. This can be avoided by a proportional reduction of the intensities. Herewith, due to the condition (14), this scaling will affect only the value of the peak area. If the scale factor is known, it is easy to restore the true value of the peak area.

## 4. Results and discussions

### 4.1. Determination of the parameter $\rho$ for the TOF mass spectrometer

To check the adequacy of the relative time channel width parameter several mass spectra were recorded at different sample rate. In the recorded mass spectra only information about  $m/z$  coordinates was used (i.e. the mass difference between adjacent points of the mass spectra). Based on this information, we have determined coefficients  $\Delta t/a$ , necessary for calculating the parameter of the relative time channel width of the detector.

Table 1 shows the values of the coefficients  $\Delta t/a$  determined by Levenberg–Marquardt method for the mass spectra recorded on Autoflex II MALDI-TOF mass spectrometer. For comparison, Table 1 also shows the value of the coefficient  $\Delta t/a$  for the mass spectra recorded on Mariner ESI-TOF mass spectrometer (PerSeptive Biosystems, Framingham, MA).

From Table 1 one can see that the change in discreteness of the mass spectrum registration leads to adequate proportional change in the value of the coefficients  $\Delta t/a$ . Coefficient  $\Delta t/a$  for Mariner is close to the value of Autoflex II at SR = 2 GS/s.

Fig. 1 shows the range of integration (the time channel width of the detector expressed in  $m/z$  units) calculated by the formula

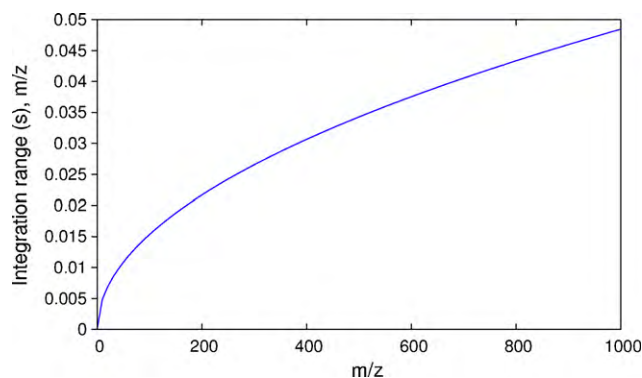


Fig. 1. The range of integration  $s(\tilde{m})$  for mass spectra recorded on Autoflex II MALDI-TOF mass spectrometer at SR = 2 GS/s.

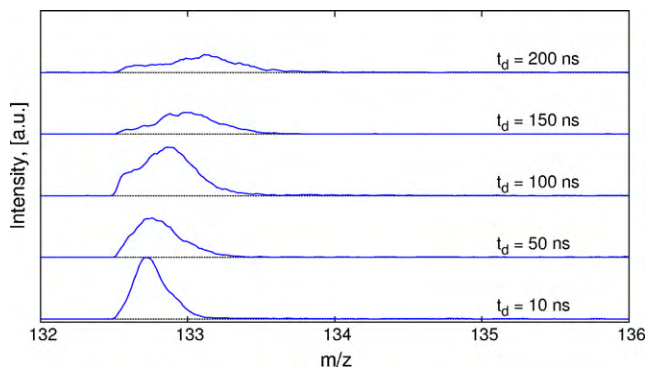


Fig. 2. Change of  $\text{Cs}^+$  peak shape depending on delayed extraction.

(13) for mass spectra recorded on Autoflex II mass spectrometer at SR = 2 GS/s.

### 4.2. Estimation of the peak areas

The use of delayed extraction of ions in MALDI [44–46] leads to a change in the distribution of initial velocities, and consequently, change the shape of the peaks. This fact was used to test the adequacy of the parameter of the peak area ( $A$ ).

Mass spectra of cesium iodide were recorded at different times of delayed extraction ( $t_d$ ): 10 ns, 50 ns, 100 ns, 150 ns and 200 ns. Fig. 2 shows the change in the shape of  $\text{Cs}^+$  peak with the increase of the delayed extraction time.

From Fig. 2 one can see that  $\text{Cs}^+$  peaks are shifted progressively in  $m/z$  towards higher values (or in time) and become broader when the delay time increases. Similar effects were noted [45,46] for the peptide mixture ACTH 7–38 and for  $\alpha$ -cyano-4-hydroxycinnamic acid.

Table 2 lists the model parameters for the peaks shown in Fig. 2. The peak area values were scaled in proportion to the maximal intensity of  $\text{Cs}^+$  peak at  $t_d = 10$  ns which was about 3248. Note, that the area of the peaks decreases with the increase of delay time due to the fast dispersion of the ablation products [47,48]. Also, detected signal becomes less smooth due to decrease in the number of ions

Table 1  
The value of coefficients  $\Delta t/a$  for TOF mass spectrometers.

Instrument	SR [GS/s]	$\Delta t/a \times 10^3 \left[ \sqrt{m/z} \right]$
Autoflex II	0.05	30.841929
	0.5	3.084193
	1.0	1.542096
	2.0	0.766215
Mariner	–	0.701097

Table 2  
The peak shape parameters of  $\text{Cs}^+$  peaks recorded at different times of delayed extraction.

$t_d$ [ns]	10	50	100	150	200
$A$	15.49	13.92	20.41	10.06	9.15
$s$	0.109	0.148	0.189	0.210	0.263
$k$	0.371	0.427	0.052	0.097	–0.171

**Table 3**The peak shape parameters of Cs<sup>+</sup> peaks recorded at different accelerating voltages.

Uis1 [kV]	20.0	19.5	19.0	18.5	18.0	17.5	17.0
$\sigma$	0.109	0.112	0.119	0.124	0.154	0.145	0.171
$k$	0.372	0.228	0.309	0.212	0.296	0.245	0.334

that are involved in the signal formation. The plume cooling results in thermalization of the ion velocities. The signature of this effect is a reduction in the asymmetry of the peaks (the  $k$  parameter) with the increase of the delayed extraction time.

#### 4.3. Estimation of the peak width

To check the adequacy of the peak width parameter ( $\sigma$ ) we systematically recorded the Cs<sup>+</sup> peak with consequent decrease of the full accelerating voltage Uis1. In TOF mass spectrometer the peak broadening associated with spread of initial velocities of the ions is inversely proportional to the accelerating voltage [38].

Table 3 summarizes the parameters of the model (12) determined in this experiment.

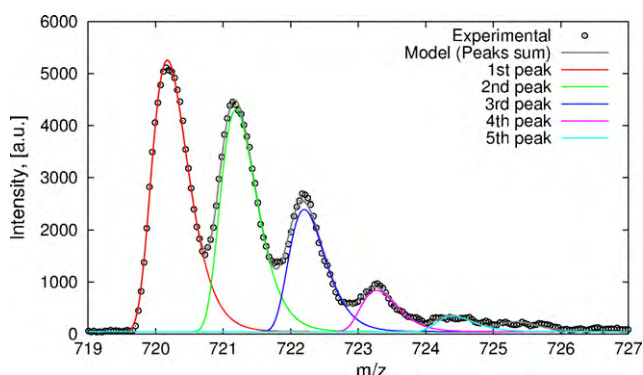
One can conclude that the peaks become broader ( $\sigma$ ) with decreasing of the full accelerating voltage. From the other side, due to the fact that the additional accelerating voltage (Uis2) changes in proportion to the full accelerating voltage (Uis1), the peak shape is almost unchanged. This is evidenced by nearly constant value of the peak asymmetry parameter ( $k$ ).

Note, that for some experimental points the data not coincide with the general trends (Uis1 = 17.5 kV in Table 3 and  $t_d = 100$  ns in Table 2). We attributed such a behavior to insufficient measurement statistics, which should be carefully controlled when performing quantitative measurements on MALDI-TOF mass spectrometers [49].

#### 4.4. Separation of the partially overlapped peaks

We applied the model (15) to separate the isotopic pattern of the fullerene C<sub>60</sub>. Results are presented on Fig. 3.

The direct use of model (15) for partially overlapped peaks does not give satisfactory results due to large number of free parameters. In this case, a minimum of the squared residuals sum may correspond to several parameter sets of model (15). To avoid such a problem one has carefully select the initial approximation which is rather tricky procedure for applied tasks. For TOF mass spectrometer the aim is somewhat simplified, because the range of integration has already been determined before fitting. This leads to a better convergence of Levenberg–Marquardt algorithm. Therefore, as an initial approximation it is enough to specify the number of peaks and their  $m/z$  for the separation of the partially overlapped peaks in the TOF mass spectra.

**Fig. 3.** Modelling of the peak shape of the isotopic pattern of fullerene C<sub>60</sub>.

## 5. Conclusions

The developed model adequately describes the shape of the peak of the experimental data. Using laser desorption mass spectra it was shown that the parameters of width and asymmetry of the peaks depend on the ion formation processes in the source.

Fitting of the experimental data by the developed model of the peak shape does not require manual selection of the approximation range and any other parameters. The proposed method does not impose any restriction on the discreteness of the mass spectrum recording.

The model can be used for both magnetic sector and TOF mass spectrometers with analog and counting detectors. In the case of time-to-digital converter for the correct estimation of peak parameters a dead-time correction should be done by the standard techniques used for this purpose (see, e.g., Ref. [43]).

## Acknowledgements

Authors are grateful to Valery Pokrovsky and Sergii Snegir (Chuiko Institute of Surface Chemistry NAS of Ukraine, Kyiv, Ukraine), and also to Yuriy Rogulsky (Institute of Applied Physics NAS of Ukraine, Sumy, Ukraine) for assistance in conducting the experiments on MALDI-TOF mass spectrometer and discussion of this work.

Also the authors thank Sergei Aksyonov (Arizona State University, Tempe, AZ, USA) for kindly providing the mass spectra of ESI-TOF mass spectrometer, as well as for numerous helpful discussions.

We are grateful to Konstantin Fedko (JSC PA ECP, Zelenogorsk, Russia) for many discussions that led us thinking about the subject of this work.

## References

- [1] J.M. Laeven, H.C. Smit, *Anal. Chim. Acta* 176 (1985) 77–104.
- [2] E.J. Breen, F.G. Hopwood, K.L. Williams, M.R. Wilkins, *Electrophoresis* 21 (2000) 2243–2251.
- [3] J.A. Falkner, M. Kachman, D.M. Vienne, A. Walker, J.R. Strahler, P.C. Andrews, *J. Am. Soc. Mass Spectrom.* 18 (2007) 850–855.
- [4] M. Mann, C.K. Meng, J.B. Fenn, *Anal. Chem.* 61 (1989) 1702–1708.
- [5] D.M. Horn, R.A. Zubarev, F.W. McLafferty, *J. Am. Soc. Mass Spectrom.* 11 (2000) 320–332.
- [6] T. Kind, O. Fiehn, *BMC Bioinformatics* 7 (2006) 234.
- [7] K. Hobby, R.T. Gallagher, P. Caldwell, I.D. Wilson, *Rapid Commun. Mass Spectrom.* 23 (2009) 219–227.
- [8] D.N. Perkins, D.J.C. Pappin, D.M. Creasy, J.S. Cottrell, *Electrophoresis* 20 (1999) 3551–3567.
- [9] F.W. McLafferty, D.A. Stauffer, S.A. Loh, C. Wesdemiotis, *J. Am. Soc. Mass Spectrom.* 10 (1999) 1229–1240.
- [10] C. Hopley, T. Bristow, A. Lubben, A. Simpson, E. Bull, K. Klagkou, J. Henrman, J. Langley, *Rapid Commun. Mass Spectrom.* 22 (2008) 1779–1786.
- [11] J.W.K. Ho, B. Morrissey, K.M. Downard, *J. Am. Soc. Mass Spectrom.* 18 (2007) 563–566.
- [12] K.C. Leptos, D.A. Sarracino, J.D. Jaffe, B. Krastins, G.M. Church, *Proteomics* 6 (2006) 1770–1782.
- [13] V.V. Raznikov, A.F. Dodonov, E.V. Lanin, *Int. J. Mass Spectrom. Ion Phys.* 25 (1977) 295–313.
- [14] V.V. Raznikov, M.O. Raznikova, *Int. J. Mass Spectrom. Ion Phys.* 63 (1985) 157–186.
- [15] D.I. Malyarenko, W.E. Cooke, B.-L. Adam, G. Malik, H. Chen, E.R. Tracy, M.W. Trosset, M. Sasinowski, O.J. Semmes, D.M. Manos, *Clin. Chem.* 51 (2005) 65–74.
- [16] M. Katajamaa, J. Miettinen, M. Orešič, *Bioinformatics* 22 (2006) 634–636.
- [17] D. Mantini, F. Petrucci, D. Pieragostino, P.D. Boccio, M.D. Nicola, C.D. Ilio, G. Federici, P. Sacchetta, S. Comani, A. Urbani, *BMC Bioinformatics* 8 (2007) 101.
- [18] R. Hussong, B.G.A. Tholey, A. Hildebrandt, *BMC Bioinformatics* 25 (2009) 1937–1943.
- [19] M. Sturm, A. Bertsch, C. Gröpl, A. Hildebrandt, R. Hussong, E. Lange, N. Pfeifer, O. Schulz-Trieglaff, A. Zerck, K. Reinert, O. Kohlbacher, *BMC Bioinformatics* 9 (2008) 163.
- [20] E. Lange, C. Gropl, K. Reinert, O. Kohlbacher, A. Hildebrandt, *Proceedings of the 11th Pacific Symposium on Biocomputing (PSB-06)*, 2006, pp. 243–254.
- [21] P. Du, G. Stolovitzky, P. Horvatovich, R. Bischoff, J. Lim, F. Suits, *Bioinformatics* 24 (2008) 1070–1077.

- [22] C.L. Gatlin-Bunai, L.H. Cazares, W.E. Cooke, O.J. Semmes, D.I. Malyarenko, J. Proteome Res. 6 (2007) 4517–4524.
- [23] D.I. Malyarenko, W.E. Cooke, E.R. Tracy, M.W. Trosset, O.J. Semmes, M. Sasinowski, D.M. Manos, Rapid Commun. Mass Spectrom. 20 (2006) 1661–1669.
- [24] P. Du, W.A. Kibbe, S.M. Lin, Bioinformatics 22 (2006) 2059–2065.
- [25] E.F. Strittmatter, N. Rodriguez, R.D. Smith, Anal. Chem. 75 (2003) 460–468.
- [26] M. Kempka, J. Sjö Dahl, A. Björk, J. Roeraade, Rapid Commun. Mass Spectrom. 18 (2004) 1208–1212.
- [27] R.A. Zubarev, P. Håkansson, B. Sandqvist, Rapid Commun. Mass Spectrom. 10 (1996) 1386–1392.
- [28] V.V. Manoilov, I.V. Zarutsky, Nauchnoye priborostroeniye (in Russian) 12 (2002) 38–46.
- [29] R.C. Eanes, R.K. Marcus, Spectrochim. Acta B 55 (2000) 403–428.
- [30] D.I. Malyarenko, W.E. Cooke, C.L. Bunai, D.M. Manos, Rapid Commun. Mass Spectrom. 24 (2010) 138–146.
- [31] V.V. Raznikov, A.R. Pikhitelev, A.F. Dodonov, M.O. Raznikova, Rapid Commun. Mass Spectrom. 15 (2001) 570–578.
- [32] V.V. Raznikov, A.R. Pikhitelev, M.O. Raznikova, Mass Spectrom. (in Russian) 3 (2006) 113–130.
- [33] O.N. Peregodov, V.A. Pokrovsky, Y.V. Rogulsky, O.M. Buhay, Mass Spectrom. (in Russian) 4 (2007) 43–48.
- [34] O.N. Peregodov, O.M. Buhay, O.A. Sidora, Instrum. Exp. Tech. 53 (2010) 247–253.
- [35] A.N. Tikhonov, V.Y. Arsenin, Solutions of Ill-posed Problems, Winston & Sons, Washington, 1977.
- [36] A.F. Verlan', V.S. Sizikov, Integral Equations: Methods, Algorithms, Programs, Nauk. dumka, Kiev, 1986 (in Russian).
- [37] V.Y. Terebigh, Introduction to the Statistical Theory of Ill-posed Problems, PHYSMATLIT, Moscow, 2005 (in Russian).
- [38] W.C. Wiley, I.H. McLaren, Rev. Sci. Instrum. 26 (1955) 1150–1157.
- [39] H. Wollnik, J. Mass Spectrom. 34 (1999) 991–1006.
- [40] A.B. Maleev, A.V. Saprygin, V.A. Kalashnikov, Y.N. Zalesov, L.N. Gall, V.D. Sachenko, A.S. Berdnikov, Y.I. Khashin, V.A. Lednyov, Ananlytica i control' 7 (2003) 362–366.
- [41] O.N. Peregodov, V.F. Shkurdoda, L.F. Sukhodub, Tech. Phys. 47 (2002) 792–793.
- [42] R.D.B. Fraser, E. Suzuki, Anal. Chem. 41 (1969) 37–39.
- [43] I.V. Chernushevich, A.V. Loboda, B.A. Thomson, J. Mass Spectrom. 36 (2001) 849–865.
- [44] P. Juhasz, M.T. Roskey, I.P. Smirnov, L.A. Haff, M.L. Vestal, S.A. Martin, Anal. Chem. 68 (1996) 941–946.
- [45] I. Fournier, A. Brunot, J.C. Tabet, G. Bolbach, Int. J. Mass Spectrom. 213 (2002) 203–215.
- [46] I. Fournier, A. Brunot, J.C. Tabet, G. Bolbach, J. Mass Spectrom. 40 (2005) 50–59.
- [47] L.V. Zhigilei, B.J. Garrison, J. Appl. Phys. 88 (2000) 1281–1298.
- [48] R. Knochenmuss, L.V. Zhigilei, J. Phys. Chem. B 109 (2005) 22947–22957.
- [49] E. Szájli, T. Fehér, K.F. Medzihradzsky, Mol. Cell. Proteomics 7 (2008) 2410–2418.